CHEMICAL ENGINEERING TRANSACTIONS

VOL. 92, 2022

A publication of AIDIC

The Italian Association of Chemical Engineering
Online at www.cetjournal.it

Guest Editors: Rubens Maciel Filho, Eliseo Ranzi, Leonardo Tognotti

ISBN 978-88-95608-90-7; **ISSN** 2283-9216

DOI: 10.3303/CET2292042

Hydrogen Production from Ethanol through Steam Reforming on Ni-based Catalysts

Sergio Iglesias-Vázquez*, José Valecillos, Leire Landa, Aingeru Remiro, Javier Bilbao, Ana G. Gayubo

Univ. of the Basque Country, Dep. of Chemical Engineering, P.O. Box 644, 48080 Bilbao, Spain
sergio.iglesias@ehu.eus

Biomass is an alternative and promising source for the sustainable production of energy and commodities such as hydrogen. For this, biomass can be converted into bioethanol through fermentation/hydrolysis that is reliably converted into hydrogen through steam reforming (SRE), and the performance of the most used catalysts for this process (Ni-based) is determined by the support components and preparation methods. In this work, three Ni-based catalysts have been compared for the SRE at 500 ºC, steam/ethanol molar ratio of 3 and a low space-time of 0.025 h^{-1} in a fluidized-bed reactor: The catalysts tested were obtained upon reduction at 850 ºC of a NiO/Al_2O_3 obtained by wetness impregnation (Ni-WI) and two spinel precursors ($NiAl_2O_4$ and $NiMgAl_2O_4$) prepared by co-precipitation (Ni-S and NiMg-S, respectively). The Ni-S and Ni-WI catalysts have similar performances with high ethanol conversion but unstable H_2 yield over time on stream, whereas the NiMg-S catalyst has a higher and more stable H_2 yield even with lower ethanol conversion, which proves differences in the prevailing reaction routes for the catalysts. The NiS and Ni-WI catalysts prompt the ethanol dehydration to ethylene (C_2H_4) on acid sites (which increases ethanol conversion) followed by its decomposition to carbon and H_2, which are prevailing routes over SR reactions, thus producing significant amount of carbon deposits, although both carbon and H_2 yield decrease suddenly after certain time on stream (TOS) due to deactivation of the C_2H_4 decomposition reaction. Conversely, the presence of MgO in the support of the NiMg-S catalyst neutralizes the acid sites and favors the ethanol steam reforming and ethanol dehydration to acetaldehyde (C_2H_4O), that is decomposed into CH_4 and CO. An overall significant amount of carbon is also deposited upon NiMg-S catalyst (from CO and CH_4 precursors) but it allows a stable behavior of the catalyst due to its filamentous nature.

1. Introduction

Energy transition to sources free of CO_2 emissions is one of the goals towards a sustainable world. One alternative to reduce CO_2 emissions is the use of hydrogen (H_2) produced from renewable raw materials as an energy vector (Mosca et al., 2020), as its energy density (122 MJ/kg) is almost three times larger than other fossil fuels (Balat and Kirtay, 2010). An interesting alternative for the sustainable H_2 production is the steam reforming of ethanol (SRE). The advantage of using ethanol is its high hydrogen content, ease to store and handle, low toxicity, free of potential catalyst poisons such as sulphur (Yoo et al., 2020) and the good perspectives for its production from lignocellulosic biomass by hydrolysis-fermentation (Aditiya et al., 2016).
SRE is an endothermic process that proceeds at relatively low temperatures (between 300 and 800 °C), with the following stoichiometry:

$$C_2H_5OH + 3H_2O \leftrightarrow 6H_2 + 2CO_2 \tag{1}$$

The use of steam/ethanol (S/E) molar ratio in the feed above the stoichiometric value (S/E = 3) improves H_2 selectivity and attenuates deactivation by coke deposition. However, the reaction mechanism is complex due to secondary reactions that take place in parallel to the steam reforming reaction and generate intermediate products and by-products, thus reducing H_2 yield. Among the secondary reactions, the following are considered (Valecillos et al., 2021):

Paper Received: 27 November 2021; Revised: 2 March 2022; Accepted: 2 May 2022
Please cite this article as: Iglesias-Vazquez S., Valecillos J., Landa L., Remiro A., Bilbao J., Gayubo A.G., 2022, Hydrogen Production from Ethanol Through Steam Reforming on Ni-based Catalysts, Chemical Engineering Transactions, 92, 247-252 DOI:10.3303/CET2292042

$$Ethanol\ decomposition: C_2H_5OH \rightarrow H_2 + CO + CH_4 \quad (2)$$

$$Ethanol\ dehydrogenation: C_2H_5OH \leftrightarrow C_2H_4O + H_2 \quad (3)$$

$$Ethanol\ dehydration: C_2H_5OH \leftrightarrow C_2H_4 + H_2O \quad (4)$$

$$Acetaldehyde\ decomposition: C_2H_4O \rightarrow CH_4 + CO \quad (5)$$

$$Acetaldehyde\ steam\ reforming: C_2H_4O + H_2O \rightarrow 3H_2 + 2CO \quad (6)$$

$$Ethylene\ steam\ reforming: C_2H_4 + 2H_2O \leftrightarrow 4H_2 + 2CO \quad (7)$$

$$Methane\ steam\ reforming\ (reverse\ of\ methanation): CH_4 + H_2O \leftrightarrow 3H_2 + CO \quad (8)$$

$$Water\ gas\ shift: CO + H_2O \leftrightarrow H_2 + CO_2 \quad (9)$$

$$Ethylene\ decomposition: C_2H_4 \rightarrow 2H_2 + 2C \quad (10)$$

$$Methane\ decomposition: CH_4 \rightarrow 2H_2 + C \quad (11)$$

$$Boudouard\ Reaction: \ 2CO \rightarrow C + CO_2 \quad (12)$$

Due to the complexity of the reaction scheme, the H_2 yield and selectivity is highly affected by reaction conditions (temperature, S/E molar ratio and space time), as well as by catalyst composition (Sharma et al, 2017). SRE has been studied both with noble and non-noble transition metal catalysts (Rh-based and Ni- and Co-based, respectively) because of their high C-C bond scission activity (Muroyama et al., 2010). Ni-based catalysts are more affordable and have a high activity for C-C bond scission, yet they promote CH_4 formation, which lowers the H_2 yield. One of the most used supports for Ni catalysts is Al_2O_3, because it has a high mechanical and thermal stability and provides a high specific surface area, improving the Ni dispersion. However, the acidity of this support leads to C_2H_4 formation through ethanol dehydration (He et al., 2019), which lowers H_2 selectivity and catalyst stability. The addition of basic substances, such as CaO or MgO, reduces the acidity of the support and decreases the metal-support interaction, thus enhancing the dispersion of the metal particles on the support (Szijjártó et al., 2013).

The catalyst preparation method affects the SRE performance. Accordingly, the synthesis of Ni/Al_2O_3 catalysts from the reduction of $NiAl_2O_4$ spinel allows incorporating large Ni loads with very good dispersion, which leads to improve the activity for the SRE (Valecillos et al. 2021). However, the acidity of the derived Al_2O_3 may cause the ethanol dehydration and promote carbon formation. In contrast, low Ni loadings should be used in the synthesis from impregnation in order to obtain an appropriate Ni dispersion. The acidity neutralization by the addition of Mg onto the support could be done in several ways. The addition by the co-precipitation method has a better performance by providing a higher surface area and Ni dispersion and enhanced SR of CH_4 in comparison with using other methods (Lee et al. 2020). Thus, the addition of Mg in a single co-precipitation step might be an interesting solution to neutralize the catalyst acidity in order to enhance the SRE performance.

This work reports the effect of the preparation method of Ni/Al_2O_3 catalysts and the addition of a basic promoter (MgO) on the conversion, products distribution and stability in the SRE reaction. To this end, three catalysts with similar Ni content have been studied: i) Ni/Al_2O_3 catalyst derived from $NiAl_2O_4$ spinel, named Ni-S; ii) Ni/Al_2O_3 catalyst derived from supported NiO/Al_2O_3 obtained by wet impregnation, named Ni-WI; and iii) Ni/Al_2O_3-MgO catalyst derived from $NiMgAl_2O_4$ spinel, named NiMg-S.

2. Materials and methods

2.1. Catalyst synthesis

The $NiAl_2O_4$ and Ni-MgO-Al_2O_3 spinel structures were synthesized by co-precipitation of nickel nitrate ($Ni(NO_3)_2\cdot 6H_2O$, Scharlau, 98%) with aluminum nitrate ($Al(NO_3)_3\cdot 9H_2O$, Panreac, 98%), and magnesium nitrate ($Mg(NO_3)_2\cdot 6H_2O$, Panreac, 98%) when applicable, using a precipitating agent (NH_4OH 0.6 M, Fluka, 5 M), according to Arandia et al., 2020 and Lee et al, 2020, respectively. The precipitating agent was added dropwise to the solution of metal precursors with 33 wt % Ni for the synthesis of $NiAl_2O_4$ spinel, and 27 wt % Ni and 20 wt % MgO for the synthesis of Ni-MgO-Al_2O_3 spinel. The precipitate was recovered by filtration and then dried at 110 ºC overnight and calcined at 850 ºC for 4 h with a ramp of 10 ºC/min. The NiO/Al_2O_3 precursor was prepared by the wet impregnation method by contacting a commercial Al_2O_3 (Alfa Aesar) with a solution of $Ni(NO_3)_2{\cdot}6H_2O$ in a rotary evaporator at 60 ºC allowing the continuous solvent evaporation. The product obtained was calcined at 600 ºC for 4 h. All three catalyst precursors were reduced at 850 ºC for 4 h in the reaction setup.

2.2. Catalyst characterization

The physicochemical properties of fresh, reduced, and deactivated catalyst samples were characterized by several techniques. Temperature-programmed reduction (TPR) (in a Micromeritics AutoChem 2920) was used to determine the number and type of reducible species in the catalysts, and their reduction temperature depending on the metal-support interactions. The density and strength of acid sites was obtained by temperature-programmed-desorption of NH_3 (NH_3-TPD) in the Micromeritics AutoChem 2920 analyzer coupled with a Pfeiffer Vacuum mass spectrometer (MS) to follow signal ms=15 of NH_3. The specific surface area and porous structure (pore volume distribution and average pore diameter) of the reduced catalysts was determined by N_2 adsorption-desorption in ASAP 2010 Micromeritics equipment at 77 K. The crystalline structure and average size of Ni crystallite (by means of the Scherrer equation) was determined by X-ray diffraction (XRD) analysis on a Bruker D8 Advance diffractometer with a CuKα1 radiation. The equipment is provided with a Germanium primary monochromator, Bragg-Brentano geometry and with a CuKα1 wavelength of 1.5406 Å, corresponding to an X-ray tube with Cu anticathode.
The amount and nature of coke deposited on deactivated catalyst samples was analyzed by temperature programmed oxidation (TPO) in a Thermo Scientific TGA Q5000TA IR thermobalance. The TPO profile (obtained from the derivative of the thermogravimetric signal (DTG)) provides information on the coke amount (area under the curve) and coke nature (location of combustion peak).

2.3. Reaction equipment and operating conditions

The kinetic runs were carried out in automated reaction equipment (Microactivity reference-PID Eng & Tech) provided with an isothermal fluidized bed reactor (22 mm internal diameter, total length of 460 mm and effective reaction length of 8 mm), connected on-line through a thermostated line to a Micro GC (Agilent 3000) with four modules for the detection and quantification of the products. A small fraction of the products stream leaving the reactor was sent to the Micro GC by means of a carrier gas (He, 15 mL min^{-1}). The atomic balance (C, H, O) is closed in all runs above 95%.
The catalytic bed consists of the catalyst (50 mg) and inert solid (25 g) (Carborundum, TECHNICAL, 105 μm, VWR Chemicals), so that the (bed height)/diameter relationship is around 2. The tests were carried out at 500 ºC, with ethanol flowrate at the inlet of 2 g h^{-1} (space time of 0.025 h^{-1}), S/E molar ratio of 3, and ethanol concentration of 5 % v/v (using a N_2 stream as an inert to dilute the gases). The upwards gas linear velocity (2.90 cm s^{-1}) is 3 times the minimum fluidization velocity.
The kinetic behavior was quantified with the following reaction indices: i) ethanol conversion (X), calculated from its molar flowrate (F) at the inlet and outlet (unreacted ethanol) of the reactor, and ii) the yield of each i product (Yi), calculated as the ratio between its molar flowrate (Fi) and the maximum molar flow-rate that can be obtained according to stoichiometry. The stoichiometric coefficient (υ_i) is 6 for H_2 (Eq(1)), 2 for CO_2, CO and CH_4 and 1 for C_2H_4O and C_2H_4 (moles of each C containing compound than can be obtained from ethanol).

$$X = \frac{F_{inlet} - F_{outlet}}{F_{inlet}} \tag{13}$$

$$Y_i = \frac{F_i}{\upsilon_i \cdot F_{inlet}} \tag{14}$$

3. Results and discussion

3.1. Catalyst properties

Table 1 summarizes the textural properties, Ni particle size, Ni content and acidity of the three reduced catalysts. The catalysts derived from spinel structures prepared by co-precipitation has higher BET surface are (especially NiMg-S) than the impregnated catalyst (Lee et al, 2020), which has higher pore size and pore volume. Both Ni/Al_2O_3 catalysts (Ni-S and Ni-WI) has a similar low but clearly measurable acidity, attributable to the same procedure used for their reduction. The acidity of the NiMg-S catalyst is negligible, which proves that the addition of MgO in the catalyst synthesis has fully neutralized the acid sites of Al_2O_3.

Table 1: Properties of the catalysts

Catalyst	S_{BET} (m^2 g^{-1})	V_{Pore} (cm^3 g^{-1})	Pore size (nm)	Ni^0 crystal size (nm)	Ni content (%)	Acidity (µmol g^{-1})
Ni-S	68.2	0.228	12.5	26	31.1	37.7
Ni-WI	54.6	0.285	19.6	44	36.6	36.9
NiMg-S	86.9	0.178	8.70	26	27.4	- -

The TPR profiles (Figure 1a) of Ni-S and NiMg-S precursors have a sole reduction peak at high temperature corresponding to the reduction of the Ni in the spinel structure. The maximum H_2 uptake for NiMg-S precursor is located at lower temperature than that of the Ni-S (800 and 900 ºC, respectively), which suggests a weaker interaction of Ni in the Ni-MgO-Al_2O_3 spinel. The profile for Ni-WI precursor profile shows two peaks; the peak at 480 ºC corresponds to the reduction of NiO_x species whereas the peak at high temperature corresponds to the reduction of Ni with strong support interaction (most probably a spinel structure). All three catalyst precursors exhibit similar total H_2 uptake due to their similar Ni content. The XRD diffractograms (Figure 1b) of Ni-S and NiMg-S precursors show peaks at 32.0º, 37.2º, 45.2º, 59.9º and 65.7º corresponding to $NiAl_2O_4$ or $MgAl_2O_4$ spinel structures. Upon reduction, two typical peaks from Ni crystals (Niº) appear at 44.6º and 52.0º, thus confirming that both catalysts consist of Ni^0 crystals supported on Al_2O_3 or Al_2O_3-MgO oxides, similarly to the Ni-WI catalyst prepared by impregnation. The crystal size of the Ni-WI catalyst (44 nm) is noticeably higher than that of Ni-S and NiMg-S catalysts (26 nm), probably due to the weaker interaction of Ni with the support in the Ni-WI catalyst, promoting the aggregation of Ni particles after reduction at high temperature (Lee et al., 2020).

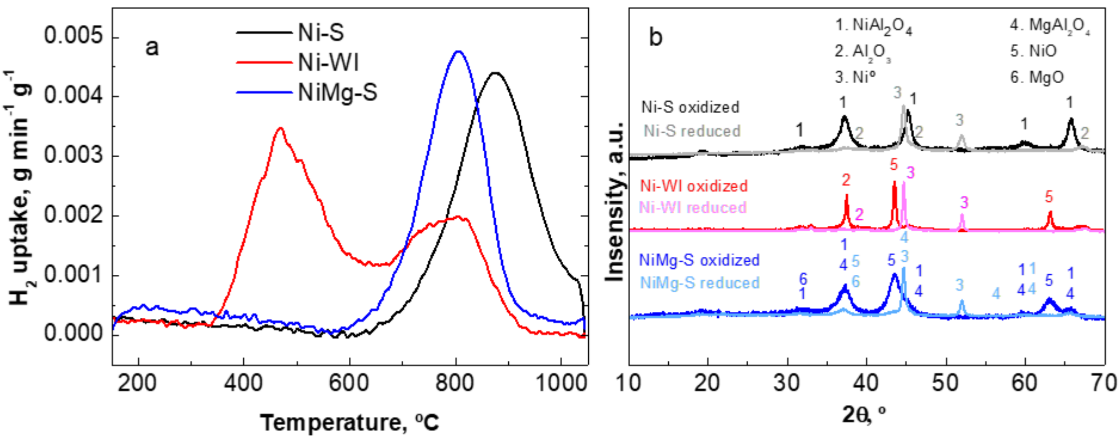

Figure 1: (a) TPR profiles and (b) XRD patterns for the three synthesized catalysts

3.2. Product distribution in SRE

The kinetic behavior in SRE of the catalysts is shown in Figure 2. Main products of all reactions are H_2, CO_2, CO, CH_4, C_2H_4 and some traces of C_2H_4O. The evolution with TOS of ethanol conversion and H_2 yield (Figure 2a) evidence similar performances for Ni-S and Ni-WI catalysts, with almost complete ethanol conversion but unstable H_2 yields that decrease towards a stationary value near 0.2 after 2 h on TOS. Conversely, NiMg-S catalyst has a higher and more stable H_2 yield, in spite of its lower ethanol conversion, which suggests different reactions routes for the acidic Ni-S and Ni-WI and non-acidic NiMg-S catalysts. Regarding carbon products (Figure 2b), Ni-S and Ni-WI catalysts promote the formation of C_2H_4 due to the Al_2O_3 acidity that catalyzes ethanol dehydration and increases the ethanol conversion. C_2H_4 decomposes rapidly into H_2 and solid carbon, which explains the high carbon yield at the beginning of the reaction for both Ni-S and Ni-WI catalysts in Figure 2b. The NiMg-S catalyst inhibits ethanol dehydration route while promoting SR reactions and ethanol dehydrogenation to C_2H_4O, which decomposes rapidly into CO and CH_4, thus explaining their similar yield. The high yields of CH_4 and CO with NiMg-S catalyst contribute to a significant solid carbon formation by CH_4 decomposition and Boudouard reactions (mainly the latter) (Montero et al., 2019). After 240 min TOS, the product distribution changed for the Ni-S and Ni-WI catalysts, being C_2H_4 the most relevant product, whereas the product distribution barely changes for the NiMg-S catalyst, demonstrating a higher stability.

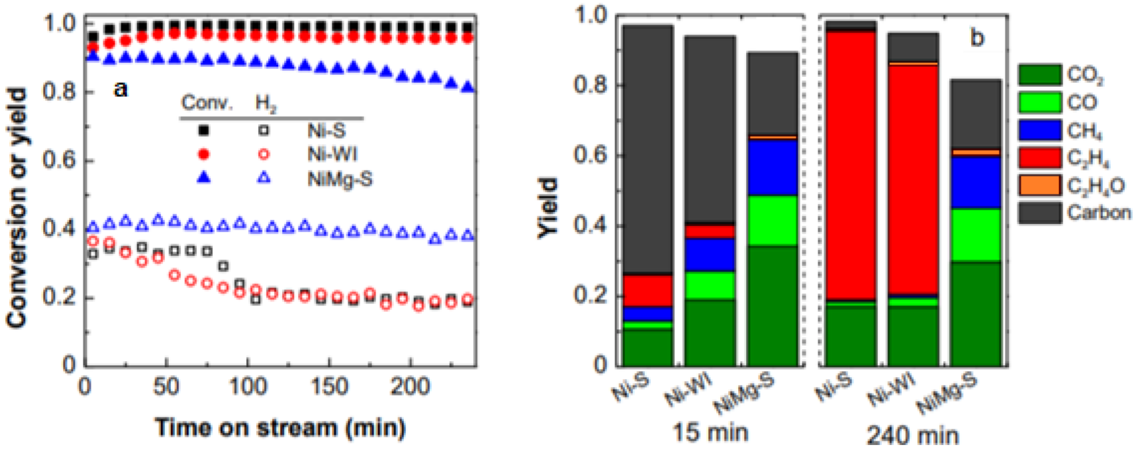

Figure 2: (a) Evolution with TOS of ethanol conversion and H_2 yield and (b) carbon product distribution at the beginning and end of each experimental run.

3.3. Quantification of solid carbon

The results of evolution of carbon yield with TOS (Figure 3a, calculated from C balance) show that there are different mechanisms of coke formation. The coke formation is very fast at the beginning of the reaction for both catalysts with acid support (Ni-S and Ni-WI) and after some TOS it decreases abruptly. That is explained because the decomposition of C_2H_4 is the main route of coke formation, which occurs at the metal-support interface, and originates carbon filaments via a tip-growth mechanism (Valecillos et al., 2021). This route is abruptly deactivated when abundant filaments accumulate and the low carbon yield observed subsequently is due to the Boudouard reaction and CH_4 decomposition (the latter with low contribution at the low reaction temperature studied). However, the carbon precursors on the NiMg-S catalyst are only CO and CH_4, both having high and stable yields, thus leading to moderate but also stable carbon yield throughout the reaction.

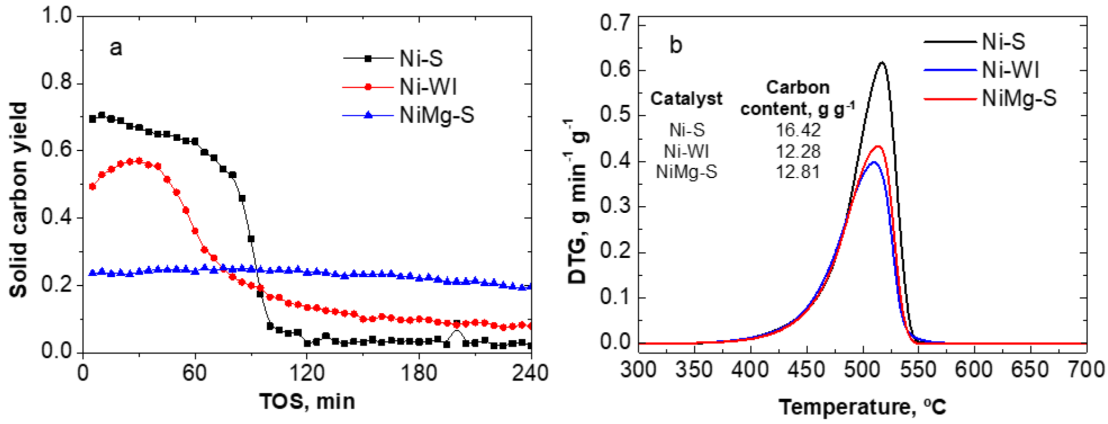

Figure 3: (a) Evolution of carbon yield with TOS and (b) TPO profiles of the carbon deposits in SRE.

The TPO profiles for the three used catalysts (Figure 3b) show a unique combustion peak with its maximum at a very similar temperature, around 513 ºC, which suggests that the carbon deposited has a similar nature, consisting of carbon filaments (Montero et al., 2019). This filamentous carbon structure explains the stable performance of NiMg-S catalyst over the whole reaction and the stable behavior of Ni-S and Ni-WI catalysts before and after the deactivation of the C_2H_4 decomposition reaction, being the only one that is severely affected by the carbon accumulation (Valecillos et al., 2021). The carbon content (Figure 3b) is slightly higher for the Ni-S catalyst, but similar for the three catalysts, which is consequence of the different coke formation dynamics: rapid at the beginning but rapidly decreasing after certain TOS for acidic supports and moderate but constant over TOS for the non-acidic support.

4. Conclusions

Three different Ni-based catalysts were studied for SRE. Two of them (Ni-S and Ni-WI) have comparable activity and product distribution, which is correlated to their similar composition and acid properties of the support. For both catalysts, the formation of C_2H_4 by ethanol dehydration on acid sites and its subsequent decomposition to carbon and H_2 prevails over SR reactions, thus producing lower yield of H_2 and undesired carbon products but a high yield of filamentous carbon at the beginning of the reaction, although the C_2H_4 decomposition reaction deactivates completely after certain TOS, causing an abrupt decrease in carbon deposition afterwards. Conversely, ethanol SR (to produce CO + H_2) and dehydrogenation (to produce C_2H_4O) are the main reaction routes in the SRE over NiMg-S catalyst, which produces a higher H_2 yield (0.41 at 500 ºC S/E=3 and space time of 0.025 h^{-1}). A high amount of carbon deposits is also accumulated over TOS with NiMg-S catalyst, whose precursors are CO and CH_4 obtained from C_2H_4O decomposition, but due to its filamentous nature it does not have a negative impact on the catalyst performance, that shows stable behavior over the whole reaction.

Acknowledgments

This work was carried out thanks to the Project RTI2018-100771-B-I00 and to the PhD grant BES-2019-090943 funded by MCIN/AEI/10.13039/ 501100011033; to the project HORIZON H2020-MSCA RISE 2018, contract 823745, funded by the European Union; and to the IT1218-19 by the Department of Education, Universities and Investigation of the Basque Government.

References

Aditiya, H.B., Mahlia, T.M.I., Chong, W.T., Nur, H. and Sebayang, A.H., 2016, Second generation bioethanol production: A critical review, Renewable and Sustainable Energy Reviews, 66, 631–653.

Arandia, A., Remiro, A., Valle, B., Bilbao, J. and Gayubo, A.G., 2020, Deactivation of Ni spinel derived catalyst during the oxidative steam reforming of raw bio-oil, Fuel, 276, 117995.

Balat, H. and Kırtay, E., 2010. Hydrogen from biomass – Present scenario and future prospects. International Journal of Hydrogen Energy, 35, 7416-7426.

He, L., Hu, S., Jiang, L., Liao, G., Zhang, L., Han, H., Chen, X., et al., 2017, Co-production of hydrogen and carbon nanotubes from the decomposition/reforming of biomass-derived organics over Ni/α-Al_2O_3 catalyst: Performance of different compounds, Fuel, 210, 307–314.

Lee, Y.L., Kim, B.J., Park, H.R., Ahn, S.Y., Kim, K.J. and Roh, H.S., 2020, Customized Ni-MgO-Al_2O_3 catalyst for carbon dioxide reforming of coke oven gas: Optimization of preparation method and co-precipitation pH, Journal of CO_2 Utilization, 4, 101354.

Lu, Y.J., Jin, H., Guo, L.J., Zhang, X.M., Cao, C.Q. and Guo, X., 2008, Hydrogen production by biomass gasification in supercritical water with a fluidized bed reactor, International Journal of Hydrogen Energy, 33, 6066–6075.

Montero, C., Remiro, A., Valle, B., Oar-Arteta, L., Bilbao, J. and Gayubo, A.G., 2019, “Origin and Nature of Coke in ethanol Steam Reforming and Its Role in Deactivation of Ni/La_2O_3-αAl_2O_3 Catalyst”, Industrial and Engineering Chemistry Research, 58, 14736–14751.

Mosca, L., Medrano Jimenez, J., Wassie, S., Gallucci, F., Palo, E., Colozzi, M., Taraschi, S. and Galdieri, G., 2020. Process design for green hydrogen production. International Journal of Hydrogen Energy, 45, 7266-7277.

Muroyama, H., Nakase, R., Matsui, T. and Eguchi, K., 2010. Ethanol steam reforming over Ni-based spinel oxide. International Journal of Hydrogen Energy, 35,1575-1581.

Ogo, S. and Sekine, Y., 2020. Recent progress in ethanol steam reforming using non-noble transition metal catalysts: A review. Fuel Processing Technology, 199, 106238.

Sharma, Y., Kumar, A., Prasad, R. and Upadhyay, S., 2017. Ethanol steam reforming for hydrogen production: Latest and effective catalyst modification strategies to minimize carbonaceous deactivation. Renewable and Sustainable Energy Reviews, 74, 89-103.

Szijjártó, G.P., Pászti, Z., Sajó, I., Erdohelyi, A., Radnóczi, G. and Tompos, A., 2013, Nature of the active sites in Ni/$MgAl_2O_4$-based catalysts designed for steam reforming of ethanol, Journal of Catalysis, 305, 290–306.

Valecillos, J., Iglesias-Vázquez, S., Landa, L., Remiro, A., Bilbao, J. and Gayubo, A.G., 2021, Insights into the reaction routes for H_2 formation in the ethanol steam reforming on a catalyst derived from $NiAl_2O_4$ spinel, Energy and Fuels, 35, 17197–17211.

Yoo, S., Park, S., Song, J.H. and Kim, D.H., 2020, Hydrogen production by the steam reforming of ethanol over K-promoted Co/Al2O3–CaO xerogel catalysts, Molecular Catalysis, 491, 110980.